AD-A124 418 DETERMINATION OF THE MICROSCOPIC STRUCTURE OF SURFACE AND OVERLAYERS ADSO..(U) CALIFORNIA INST OF TECH PASADENA W H WEINBERG 28 DEC 82 P-13120-C/P-16273-C 1/1

UNCLASSIFIED ARO-16273.6-CH DAAG29-79-C-0132 F/G 20/2 NL

END

DATE FILMED

83

DTIC

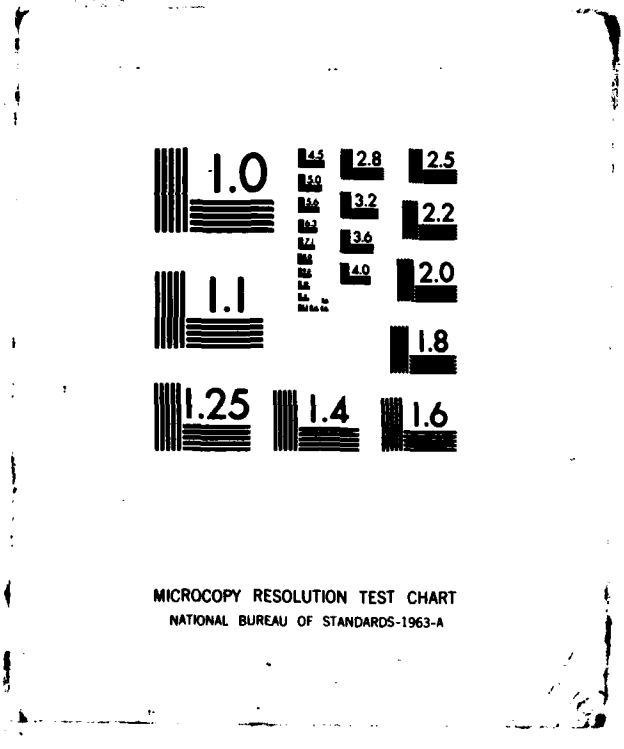

ARO 16273.6-C

REPORT DOCUMENTATION PAGE

READ INSTRUCTIONS BEFORE COMPLETING FORM

1. REPORT NUMBER: P-13120-C/P-16273-C
2. GOVT ACCESSION NO.: AD-A124418
3. RECIPIENT'S CATALOG NUMBER:

4. TITLE (and Subtitle): Determination of the Microscopic Structure of Surfaces & Overlayers, Adsorbate-Adsorbate Interaction Energies, & Rates of Surface Processes
5. TYPE OF REPORT & PERIOD COVERED: Final 9/25/79-9/24/82
6. PERFORMING ORG. REPORT NUMBER:

7. AUTHOR(s): W. Henry Weinberg
8. CONTRACT OR GRANT NUMBER(s): DAAG29-79-C-0132

9. PERFORMING ORGANIZATION NAME AND ADDRESS: California Institute of Technology, 206-41, 1201 E. California Blvd., Pasadena, CA 91125
10. PROGRAM ELEMENT, PROJECT, TASK AREA & WORK UNIT NUMBERS:

11. CONTROLLING OFFICE NAME AND ADDRESS: U.S. Army Research Office, P.O. Box 12211, Research Triangle Park, N.C. 27709
12. REPORT DATE: 12/28/82
13. NUMBER OF PAGES:

14. MONITORING AGENCY NAME & ADDRESS (if different from Controlling Office)
15. SECURITY CLASS. (of this report): Unclassified
15a. DECLASSIFICATION DOWNGRADING SCHEDULE:

16. DISTRIBUTION STATEMENT (of this Report)

Approved for public release; distribution unlimited.

17. DISTRIBUTION STATEMENT (of the abstract entered in Block 20, if different from Report)

N/A

DTIC ELECTE S FEB 15 1983 D E

18. SUPPLEMENTARY NOTES

The view, opinions, and/or findings contained in this report are those of the author(s) and should not be construed as an official Department of the Army position, policy, or decision, unless so designated by other documentation.

19. KEY WORDS (Continue on reverse side if necessary and identify by block number)

Surface processes, surface reactions, surface crystallography, molecular beam-surface scattering, high pressure microreactor, heterogeneous catalysis.

20. ABSTRACT (Continue on reverse side if necessary and identify by block number)

Progress has occurred in three major areas with the support of ARO Contract DAAG29-79-C-0132. First, work has continued in the general area of surface crystallography making use of low-energy electron diffraction. Second, a supersonic nozzle ultrahigh vacuum molecular beam surface scattering machine has been designed and constructed. This extremely versatile instrument allows precise measurement of a wide variety of surface phemonena including the elementary steps in gas-solid chemical reactions. Finally, a high pressure

p.

DD FORM 1 JAN 73 1473 EDITION OF 1 NOV 65 IS OBSOLETE

unclassified

Table of Contents

I. Introduction

Progress has occurred in three major areas with the support of ARO Contract DAAG29-79-C-0132. First, work has continued in the general area of surface crystallography, making use of low-energy electron diffraction. Second, a supersonic nozzle ultrahigh vacuum molecular beam surface scattering machine has been designed and constructed. This extremely versatile instrument allows precise measurement of a wide variety of surface phenomena, including the elementary steps in gas-solid chemical reactions. Finally, a high pressure microreactor has been designed and constructed. This microreactor will be a useful adjunct to the molecular beam machine since in the former overall reaction kinetics will be measured under realistic pressure conditions, whereas in the latter elementary reaction rates will be measured under conditions of low pressure. Each of these three projects is described in more detail below.

II. Surface Crystallography

Insofar as our work in low-energy electron diffraction (LEED) is concerned, a more sensible reliability (R-) factor has been formulated in order to compare quantitatively calculated and measured LEED intensity-voltage (I-V) beam profiles (1). Furthermore, a photographic method was developed which allows a precise determination of both the polar and azimuthal angles of incidence in a LEED experiment (2). In this connection, an equation was developed to describe the geometrical relationships between the electron gun, the crystal surface, and the phosphorescent display screen in back-reflection, post-acceleration LEED experiments. Photographic methods for determining the polar and azimuthal angles of incidence in LEED experiments

can be derived starting from this equation. In particular, two published procedures appear here as special cases. New methods are described for cases where the existing techniques do not apply. It is shown that the alignment of the electron gun and the positioning of the crystal can be checked using a photographic technique. An example illustrates that the angles of incidence can be measured with precisions of $\pm 0.2^{o}$ by recording data on several photographs taken over a wide range in electron energy.

In an attempt to determine the influence of the presence of adjacent islands on LEED beam profiles, an excluded area model was proposed to describe the relative positions of ordered islands on a crystal surface (3,4). On the basis of this model, overlayers of different island density were created on a finite lattice using a simple computer algorithm. The LEED intensity from these overlayers was calculated kinematically. Although the placement of the islands is not random, this does not perturb the LEED beam profile observably. Therefore, the kinematically diffracted intensity depends solely on the distribution of island size. Using this result, the intensity and half-width as functions of coverage were calculated for one model of island growth. In addition, the formation and dissolution if islands of CO on Ru(001) was investigated both theoretically and experimentally (5,6).

III. Design and Construction of a High Pressure Catalytic Microreactor

A microreactor has been designed and constructed to obtain information concerning heterogeneous reactions of gaseous reactants on metal and metal oxide surfaces. The major design considerations were to make the volume as small as possible and to have a method of cleaning the catalytic surface (an

iron foil, an iron single crystal or an oxidized surface of either) prior to reaction. Minimizing the volume increases the ratio of catalytic surface area to total gas volume and, consequently, increases sensitivity. The manner by which either the surface of the single crystalline sample or the polycrystalline foil can be cleaned will be determined initially in the UHV system described in Section IV using thermal He beam scattering, Auger spectroscopy, XPS and LEED. Identical cleaning procedures will then be carried out in the microreactor with quantitative thermal desorption spectra of H_2 and CO used as an additional gauge of a clean surface.

The microreactor consists of two major components: a manipulator with which the crystal can be translated and rotated, and a main body where reactions and cleaning occur. These and other features of the microreactor are described below.

The crystal manipulator, adapted from a design of Auerbach et al (7), consists of a doubly differentially pumped housing, a shaft which supports the crystal, and three spring loaded teflon O-rings which allow the shaft to be translated and rotated. A schematic of the manipulator is shown in Fig. 1. The housing is a stainless steel tube which contains the O-rings and is welded to a 2-3/4" flange for attachment to the reactor body. Two stainless steel rings separate the O-rings and align them with two 3/16" pump-out ports. A removable top plate secures the O-rings in the housing. The first port is pumped by a mechanical pump, while the second section will use a Varian 2" diffusion pump with a chilled water-cooled baffle.

A mini-feedthrough (Ceramaseal 807B9299-2), welded to a stainless steel tube, comprises the shaft. This shaft provides support for the crystal or foil via two 0.051" OFHC copper wires which are used also to heat the sample.

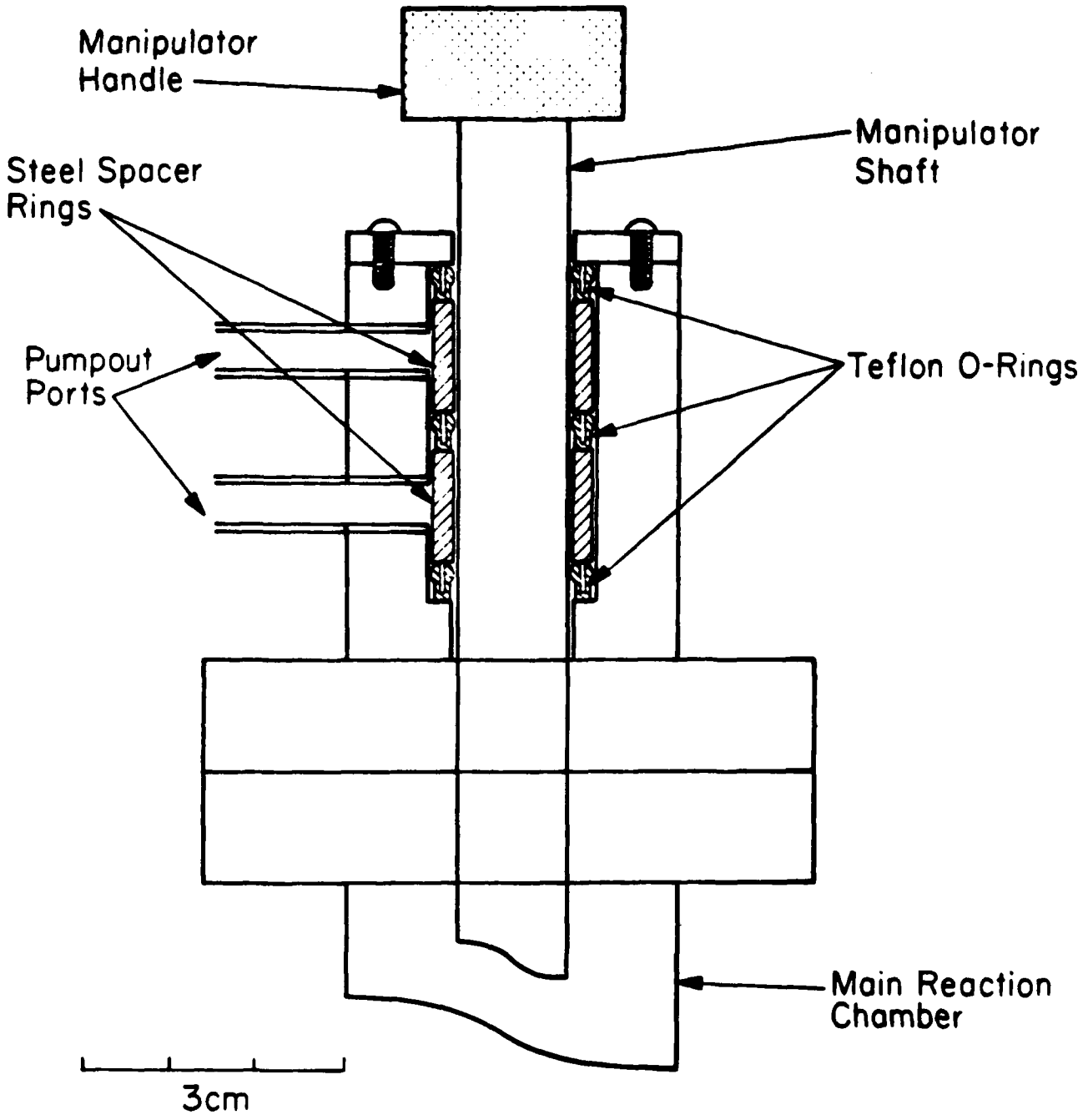

Figure 1: Cross Section of Manipulator for High Pressure System.

Thermocouple wires are attached for temperature measurement. Cooling is achieved by filling the hollow shaft with liquid nitrogen. Spring loaded teflon O-rings (Accratronics Ar10400-206AC) are used to form a seal between the shaft and the manipulator housing. The shaft can be translated and rotated while maintaining a seal. All sealing surfaces have been machined to obtain an optimum metal-to-teflon seal.

Leakage past the O-rings and the degree to which the base pressure in the system is limited by this leakage is calculated as follows. The pressure before a seal, P_a, is related to the pressure after the seal, P_b, by

$$P_a L = S P_b \qquad (1)$$

where L is the leak rate of the seal, and S is the speed at which gases are pumped away. The typical leak rate of a 14" diameter seal is stated by Auerbach et al (7) to be 10^{-6} l/sec. This corresponds to 3.6×10^{-8} l/sec for a 1/2" diameter seal. Assuming atmospheric pressure before the first seal and a pumping speed of 10^{-3} l/sec (certainly a lower limit), the pressure in the first chamber would be 2.7×10^{-2} Torr. Assuming the same pumping speeds in the second chamber and main reactor body results in a base pressure due to leakage below 3.5×10^{-11} Torr in the main chamber. Since this is below current limitations due to other factors, seal leakage does not and will not limit the base pressure of the system.

The main chamber of the microreactor consists of a right-angle ultra-high vacuum valve which has been modified by replacing the port opposite the bellows with a tube of 13/16" internal diameter, as shown in Fig. 2. This diameter is just large enough to accommodate the manipulator shaft, resulting in a volume of 10.2 cm^3. Access to the chamber is through four 3/16" ports spaced 90^o apart.

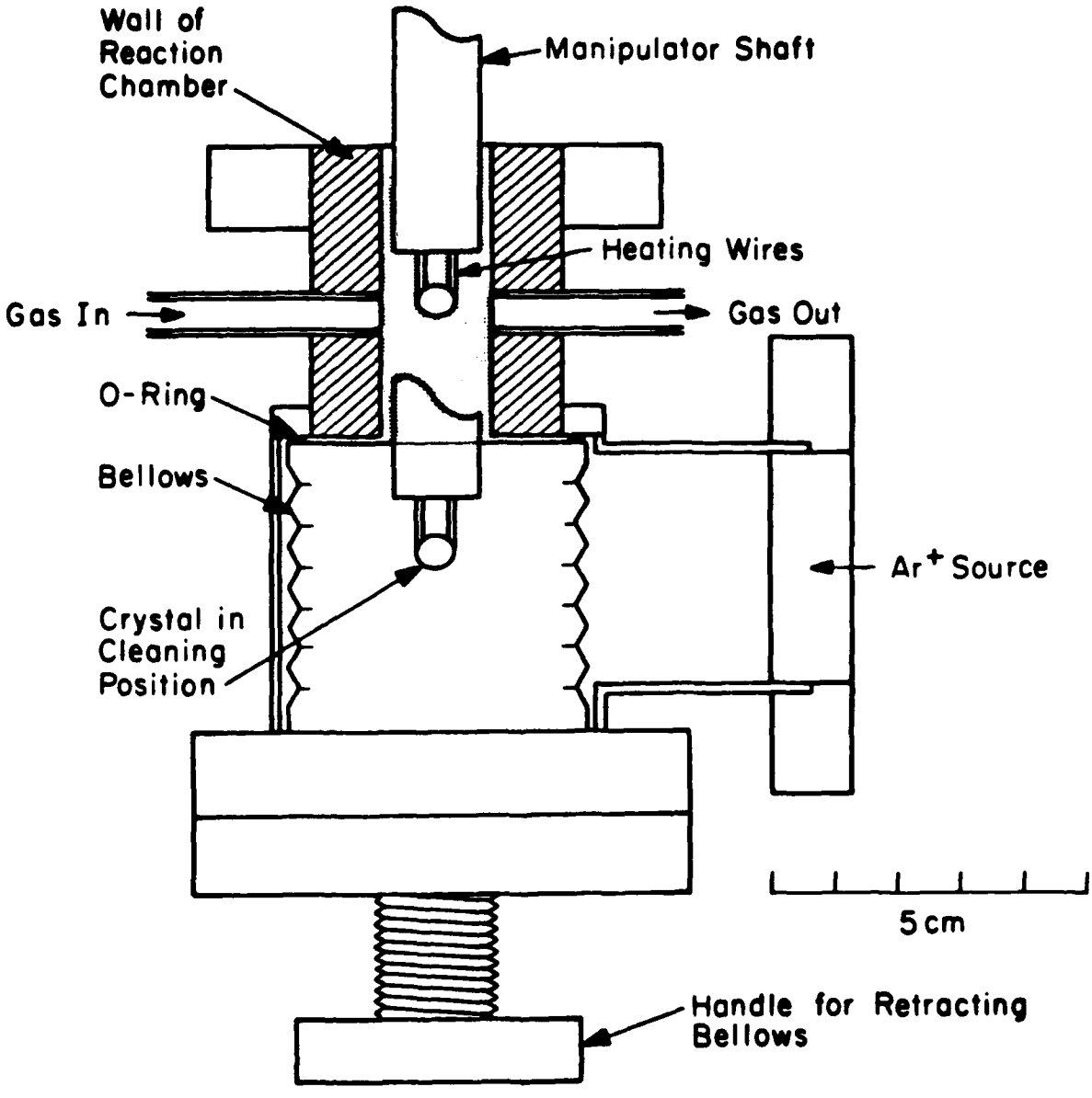

Figure 2: Diagram of main microreactor body showing the crystal both in the high pressure and the cleaning positions. The shaded area is the reaction volume, 10.2 cm^3.

With this design, the crystal may be cleaned by rare gas ion bombardment or sealed inside the chamber of the microreactor. To clean the crystal, the right-angle UHV valve is opened and the crystal is translated until it faces the rare gas ion beam. Both sides of the crystal may be cleaned by rotating it 180^{o}. When carrying out a high pressure reaction, the crystal is positioned in the reaction chamber, and the right-angle UHV valve is closed. This arrangement maintains the rest of the system containing the ion gun and mass spectrometer under vacuum while the reaction is carried out. Surfaces which are exposed to high pressures have been plated with $\sim .5 \times 10^{-5}$ inch of gold to suppress any reaction from occurring on the chamber walls. The region containing the mass spectrometer is currently pumped with a Varian 2" diffusion pump with a chilled water baffle (90 l/sec). The current base pressure of the all-metal, bakeable microreactor is in the low 10^{-8} Torr range, but it can be lowered into the UHV range by the addition of a cryotrap.

Product concentrations will be detected by two methods: gas chromatography and mass spectrometry. The outlet flow of the reactor is coupled to a Bendix 2500 gas chromatograph (GC) which has both flame ionization and thermal conductivity detectors. A variety of columns will be used depending on the species being analyzed. The second method of detection is a differentially pumped quadrupole mass spectrometer (EAI 1200) which is linked to the microreactor chamber via interchangeable pieces of capillary tubing (Wilmad Glass Co.), the inside diameters of which vary from 0.001" to 0.004". The length has been made sufficiently short, 0.5 cm, to avoid any separation within the capillary. Conductance calculations show that with this range of diameters, a pressure of 10^{-5} Torr can be maintained at the mass spectrometer with a pressure of 1 to 760 Torr in the microreactor chamber.

Although detection limits for the GC have not been calculated, Goodman et al (8) have reported that the desorption of a monolayer of methane from a surface, the area of which is 1 cm^2, into a volume, the extent of which is 100 cm^3, can be observed easily with a flame ionization detector. The desorption of one monolayer at a total pressure of 1 Torr is detectable quantitatively by the mass spectrometer.

The microreactor will be operated both in a steady flow and in a batch mode. In the latter case, conversion will be kept sufficiently low to ensure differential operation of the microreactor. Calibrated metering valves on the inlet and outlet streams determine the flow rate. Flow rates from 0.1 to 100 cm^3/sec are possible over a wide range of pressures. Average residence times for gas molecules with these flow rates lie between 100 and 0.1 sec.

IV. Design and Construction of a Supersonic Nozzle Beam-Surface Scattering Machine

A supersonic nozzle molecular beam coupled to an UHV chamber has been constructed in our laboratory. The design and construction of this machine has involved a considerable investment of time (approximately three years) and money (approximately $460,000). The design of the apparatus stresses versatility while retaining modularity and compactness.

The molecular beam part of the system consists of a nozzle-skimmer chamber and two collimating buffer chambers as shown in Fig. 3. The nozzle-skimmer chamber is pumped by an Edwards booster oil diffusion pump having a pumping speed of 500 l/sec at 10^{-1} Torr background pressure. The nozzle itself is mounted on a high pressure xyz translator with a positioning

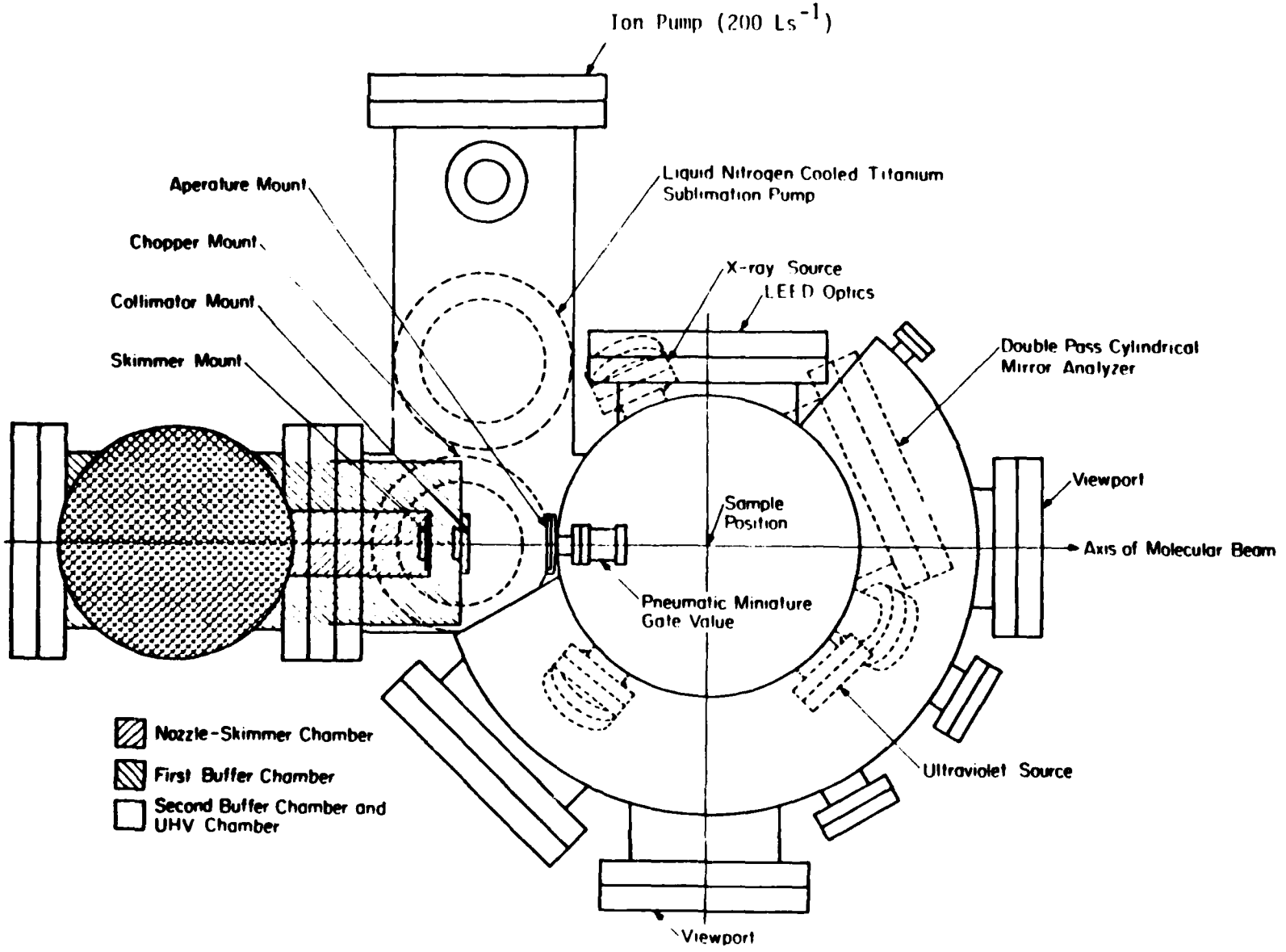

Figure 3: Cross Section of Molecular Beam.

accuracy of ±5 microns. Provision has been made to allow liquid nitrogen cooling or resistive heating of the nozzle tip. The nozzle-to-crystal sample distance has been kept as short as possible, namely, 25 cm.

A high pressure of gas (approximately 10-50 atmospheres) expands through the small orifice in the tip of the nozzle (the diameter of which is variable between 5 and 1000 microns). The expansion results in an intense beam of molecules, characterized by a narrow velocity distribution, in a collisionless flow environment. Cooling of the gas during the expansion affects the population of the translational, the rotational and the vibrational levels. The resulting population distribution can be estimated using the parameters of the source, i.e. the pressure, the temperature and the size of the nozzle orifice.

The beam is designed to allow the option of operating at rather high pressures in the first chamber. According to Camparague (9), the shock wave generated by the hydrodynamic expansion of the gas from the nozzle protects the emergent beam from the background gas when the skimmer is positioned properly with respect to the nozzle. The advantage of this technique is the ability to use high stagnation pressures, resulting in high Mach numbers, high fluxes at the crystal and quite narrow velocity distributions. For example, calculations indicate that for a stagnation pressure of 50 atmospheres of CO, a 25 micron nozzle diameter and 0.5 mm skimmer and collimating apertures, the flux at the crystal will be approximately 2×10^{15} molecules/cm^2-sec. The value of $\Delta v/v$ (an index of the monochromaticity of the velocity of the beam) is on the order of 5% with a Mach number of approximately 30 in this case. On the other hand, $\Delta v/v$ for He should be below 2% with a Mach number greater than 75 under similar conditions in our apparatus.

The first buffer chamber is pumped with an Edwards "Diffstak" oil diffusion pump with a pumping speed of approximately 700 l/sec at the 10^{-5} Torr background pressure estimated for this chamber when operating the beam. The nozzle-skimmer chamber and the first buffer chamber are embodied in a single modified 6" cross vacuum fitting which is completely demountable from the UHV chamber. The second buffer chamber is integral to the UHV system proper as shown in Fig. 3. The last chamber (the second buffer chamber) houses a mechanical chopper for the incident beam and is differentially pumped by a 200 l/sec Ultek ion pump (which should be replaced by a turbomolecular pump for more effective pumping of rare gases). The background pressure in this stage should be in the low 10^{-8} Torr range when the beam is operating. The third beam chamber can be isolated from the UHV chamber by a mini-UHV gate valve.

The main UHV chamber consists of three levels as shown in Fig. 4, but it is only 5' in height and has a volume of only about 100 liters. The main chamber is pumped principally by a 2000 l/sec turbomolecular pump with auxiliary 200 l/sec of ion pumping and a liquid nitrogen cooled titanium sublimation pump. The base pressure of the main chamber is estimated to be approximately 3×10^{-11} Torr with the pressure rising into the high 10^{-10} to low 10^{-9} Torr range when the beam is operating, depending on the conditions of operation. After a mild bakeout (125°C), the current main chamber pressure is already below 2×10^{-10} Torr.

The top level, a modified vacuum coupling, is mounted on top of a UHV gate valve which can isolate it from the main chamber. The coupling is designed to be used as a high pressure crystal processing (e.g. oxidation or reduction) system, and it may also serve as a quick access port for

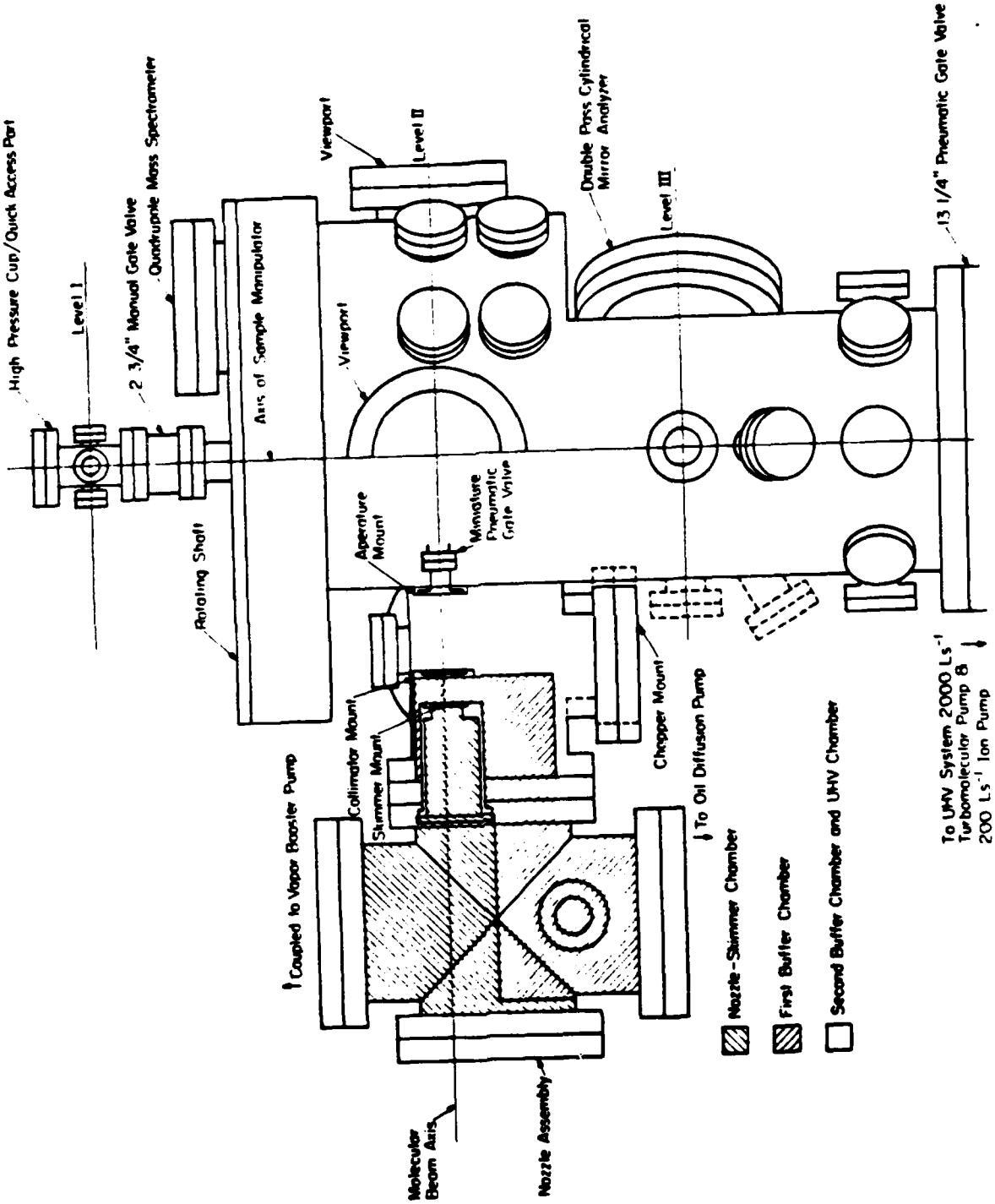

Figure 4: Molecular Beam Ultrahigh Vacuum Apparatus.

retrieving (introducing) the sample from (to) the main chamber. The second level is designed for molecular beam experiments. The molecular beam enters the main chamber at this level and is focused on the sample at the center of the bell jar. Low-energy electron diffraction (LEED) optics are also mounted on this level. A double-pass cylindrical mirror kinetic energy analyzer is mounted on the third level for photoemission and Auger spectroscopic measurements. Although only Auger electron spectroscopy is included at the moment, provision has been made to add an X-ray source (for XPS) and a UV lamp (for UPS) to the system as soon as possible.

The third beam chamber intrudes 4" into the bell jar on the second level. This level consists of a 210^{o} arc of 9" radius which truncates to a 5" radius in the remaining 150^{o}. This truncation permits LEED optics to be mounted on this level allowing selection of a particular azimuth for a scattering experiment and, in addition, reduces the total volume of the system to be pumped.

The extended 9" radius of the bell jar allows the positioning of a rotatable EXTRANUCLEAR quadrupole mass spectrometer detector at a crystal surface-to-ionizer distance of 15 cm, providing acceptable resolution for time-of-flight scattering measurements. A bakable, UHV compatible mechanical chopper will be mounted on this level within the main UHV chamber to allow postscattering beam modulation. The quadrupole mass spectrometer is rotatable by virtue of a doubly differentially pumped rotating shaft 18" in diameter, sealed with spring loaded teflon O-rings, following the design of Auerbach et al (7). This comprises the lid of the bell jar itself and is shown in cross section in Fig. 5. Calculations indicate that the leak across this seal is a negligible load on the vacuum chamber (below 10^{-13} Torr-l/sec), and no pressure rise has been found (at the 2×10^{-10} Torr

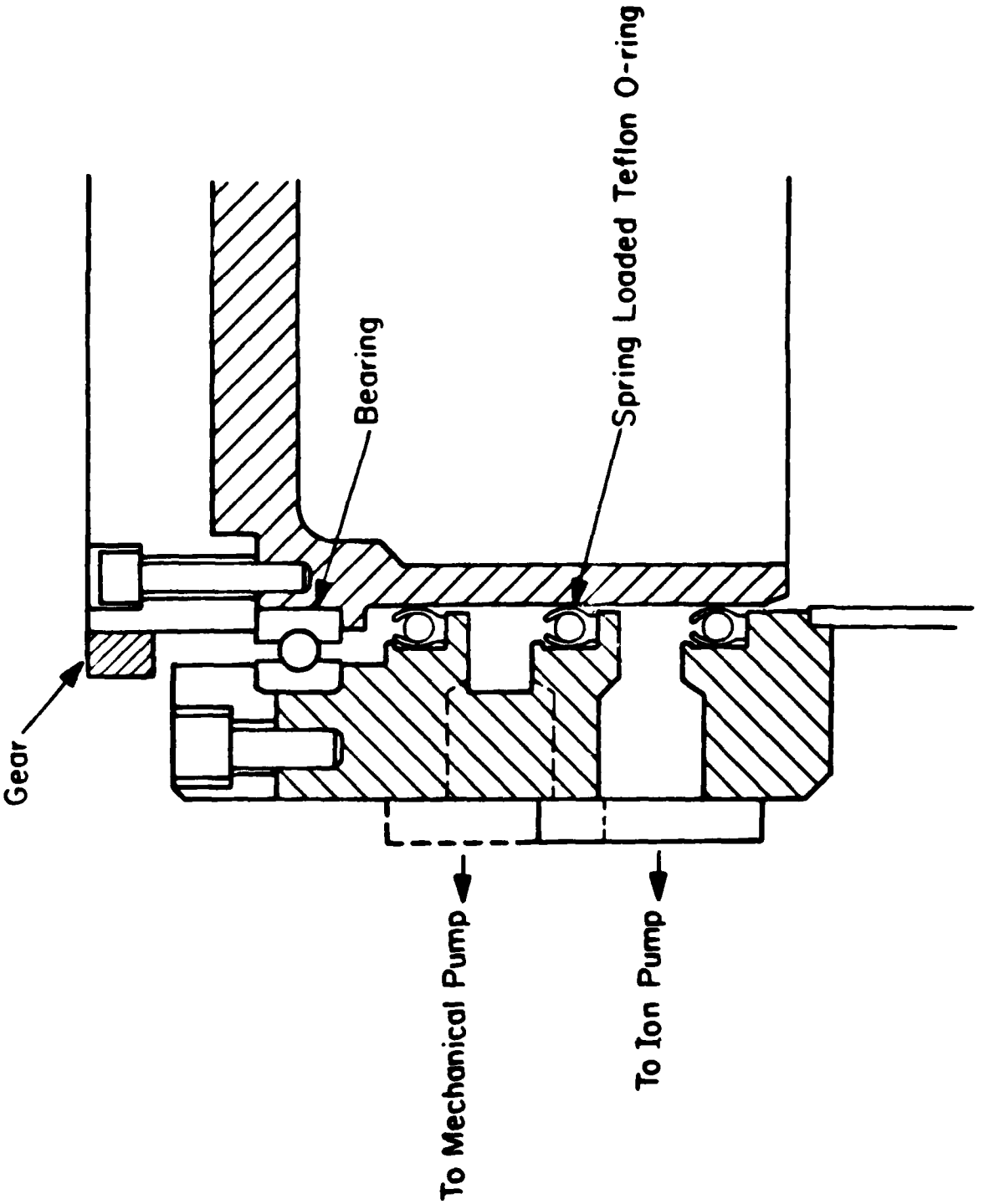

Figure 5: Cross Section of Dynamic Seal.

level) upon rotation of the seal. A design for double differential pumping of the quadrupole mass spectrometric detector has just been finalized. This differential pumping will be necessary both to observe weak diffraction beams from surfaces with a smooth corrugation function (e.g. the [111] azimuth of the Fe(211) surface) and to probe reactive scattering where the probability of reaction is small (e.g. $<10^{-2}$). The differential pumping sheath will include also two collimating apertures (of variable diameter) in order to define the angular resolution (typically $\lesssim 1^{o}$) for measuring the angular distributions of the scattered species. The free rotation of the quadrupole extends for approximately 180^{o} from 30^{o} forward of the incident beam through the path of the directly incident beam on the far side of the chamber, allowing the velocity distribution of the directly incident beam to be characterized. The mass spectrometer is interfaced already to the pulse counting electronics of a programmable multichannel analyzer for data acquisition and analysis. A plot of the intensity of the scattered molecules as a function of flight time from the chopper to the detector is obtained experimentally. This time-of-flight spectrum is transformed to velocity coordinates and compared to the velocity distribution of the beam when it does not scatter from the sample.

The bell jar truncates completely to a 5" radius at the lowest (third) level where facilities for Auger electron spectroscopy (and the subsequent addition of XPS and UPS) are included. With these spectroscopic techniques, the iron surface can be well characterized with respect to the presence of impurities, and information concerning the bonding of adsorbates on the surface may be obtained. In conjunction with LEED and thermal He beam scattering, these spectroscopic techniques can be used to ensure that the surface is clean and well ordered, or, in cases where the surface is modified,

that either a particular adsorbate is present with a known concentration or that the surface is in a particular state of oxidation. Alternatively, if changes occur in the scattering data over the period of measurement, the beam experiment can be terminated and the state of the surface investigated.

Finally, the iron crystal to be studied is mounted on a high precision xyz manipulator capable of 360° of rotary motion as well as azimuthal rotation. The crystal can be cooled to below 80 K with liquid nitrogen or heated resistively to the phase transition temperature of iron. The total travel of the manipulator is 50 cm.

References

1. A. C. Sobrero and W. H. Weinberg, in Proceedings of Conf. on Determination of Surface Structures by LEED, Plenum, N.Y., 1983.

2. A. C. Sobrero and W. H. Weinberg, Rev. Sci. Instrum. 53, 1566 (1982).

3. E. D. Williams and W. H. Weinberg, in Proceedings of 4th Internal. Conf. on Solid Surfaces, Cannes, 1980, p. 311.

4. E. D. Williams and W. H. Weinberg, Surface Sci. 109, 574 (1981).

5. E. D. Williams and W. H. Weinberg, J. Vacuum Sci. Technol. 20, 534 (1982).

6. E. D. Williams, W. H. Weinberg and A. C. Sobrero, J. Chem. Phys. 76, 1150 (1982).

7. D. J. Auerbach, C. A. Becker, J. P. Cowin and L. Wharton, Rev. Sci. Instrum. 49, 1518 (1978).

8. D. N. Goodman, R. D. Kelley, T. E. Madey and J. T. Yates, Jr., J. Catal. 63, 226 (1980).

9. R. Camparague, J. Chem. Phys. 52, 1795 (1970).

List of Publications Supported by ARO Contract DAAG29-79-C-0132

1. E. D. Williams and W. H. Weinberg, in Proceedings of 4th Internal. Conf. on Solid Surfaces, Cannes, 1980, p. 311.

2. E. D. Williams and W. H. Weinberg, Surface Sci. 109, 574 (1981).

3. E. D. Williams and W. H. Weinberg, J. Vacuum Sci. Technol. 20, 534 (1982).

4. E. D. Williams, W. H. Weinberg and A. C. Sobrero, J. Chem. Phys. 76, 1150 (1982).

5. A. C. Sobrero and W. H. Weinberg, Rev. Sci. Instrum. 53, 1566 (1982).

6. A. C. Sobrero and W. H. Weinberg, in Proceedings of Conf. On Determination of Surface Structures by LEED, Plenum, N.Y., 1983.

Scientific Personnel

1.	A. C. Sobrero	PhD. Student	
2.	J. Vajo	"	
3.	E. Williams	"	(degree granted 9/81)
4.	J. Zinck	"	
5.	W. H. Weinberg	Professor	

APPENDIX

Reprints of Published Papers